Arsenate removal with 3-mercaptopropanoic acid-coated Superparamagnetic Iron Oxide Nanoparticles

D.MORILLO[a], A.UHEIDA[b], G. PÉREZ[a], M. MUHAMMED[b] and M. VALIENTE[a]*

[a]*Universitat Autònoma de Barcelona, Centre GTS, Department of Chemistry, 08193 Bellaterra (Barcelona), Spain, Diego.morillo.martin@gmail.com, Gustavo.perez@uab.es and manuel.valiente@uab.cat*,*

[b]*Royal Institute of Technology (KTH), Functional Materials Division, 16440 Kista (Stochkolm), Sweden, salam@kth.se and mamoun@kth.se.*

* Corresponding Author

ABSTRACT

In the present work, superparamagnetic iron oxide nanoparticles (SPION) surface-coated with 3-mercaptopropanoic acid (3-MPA) were prepared and their feasibility for the removal of arsenate from dilute aqueous solutions was demonstrated. The synthesized 3-MPA-coated SPION was characterized using transmission electron microscopy (TEM), thermogravimetric analysis (TGA) and Fourier transform infra-red spectrometry (FTIR). Separation efficiency of the coated nanoparticles and the equilibrium isotherm of arsenate adsorption were investigated. The obtained results reveal the arsenate adsorption to be highly pH-dependent, and the maximum adsorption was attained in less than 60 minutes. The resulting increase of 3-MPA-coated SPION adsorption capacity to twice the adsorption capacity of SPION alone under the same conditions is attributed to the increase of active adsorption sites. An adsorption reaction is proposed. On the other hand, efficient recovery of arsenate from the loaded nanoparticles was achieved using nitric acid (HNO_3) solution, which also provides a concentration over the original arsenate solution.

1

HIGHLIGHTS

- Feasibility of using SPION modified with 3MPA for the removal of As(V).

- The adsorbent system results in an effective sorption for selective As(V) removal.

- The adsorption capacity for As(V) is higher comparing with other adsorbent systems**.**

- Adsorption mechanism has been proposed as the most suitable considering the results.

KEYWORDS

Arsenate removal, Superparamagnetic Iron Oxide Nanoparticles, SPION, 3-mercaptopropionic acid.

1. Introduction

Arsenic is a relatively scarce element in the environment atmosphere, water, soil and organisms. Usually it exists combined with other elements, for example, with sulphur, oxygen and iron and the arsenic species toxicity depends on its oxidation state, being As(-III) the most toxic specie [1]. The World Health Organization (WHO) has reduced the Maximum Contamination Level (MCL) from 50 µg/L to 10 µg/L. Therefore, it is noteworthy that the continuous regulations strengthening make necessary the improvement of existing arsenic remediation methods. [2,3].

A great variety of water treatment methodologies s such as precipitation [4], oxidation [5], liquid-liquid extraction [6,7], ion exchange [8], membrane processes [9], surface complexation [10] and selective adsorption [11,12] have been studied for significant reduction or remove arsenic from contaminated effluents.

The essence of nanoscience and nanotechnology is the ability to create materials, structures and systems which exhibit new properties for novel applications, a combination of the desired properties and functionalities is achieved at nanometer scale [13]. Small size gives nanoparticles a high surface area to volume ratio, a high surface reactivity, new properties such as magnetic, chemical etc…. In this sense, the interaction with different kinds of chemical species offers better kinetics for selective sorption of ions from aqueous solutions [14]. Highly reactive nanoparticles such as nanosized sorbents have been developed specifically to remediate contamination by heavy metal ion contaminants [15,16]. Nanoparticles (10–500 nm) provide an opportunity to deliver these remedial agents to subsurface contaminants in situ, and provide access to contamination trapped in the smallest pores in an aquifer matrix.

At the nanoscale, inorganic metal oxides are potentially highly efficient agents for binding ions such as arsenic or some pollutants and today's challenge is the translation of these achievements into an industrial production environment which requires scale-up to a continuous and safe nanoparticle

manufacturing process as reported elsewhere [17-19]. By tailoring the composition of the metal oxides, selective adsorption of different ions can be introduced. The utilization of nanoparticles for the recovery of metal ions from industrial wastes or natural water effluents has proved itself as superior new process.

In the present study the feasibility of using SPION coated with 3-mercaptopropionic acid is demonstrated for selective sorption of arsenate from aqueous solutions and an adsorption mechanism has been proposed as the most suitable considering the obtained results throughout the study. The sorption properties were studied under static mode of operation.

2. Experimental section

2.1. Chemicals and Reagents

Stock solutions of As(V) were prepared from $Na_2HAsO_4 \cdot 7H_2O$ (Sigma-Aldrich). Analytical grade $FeCl_2 \cdot 4H_2O$, $FeCl_3 \cdot 6H_2O$ (Sigma-Aldrich), ammonium hydroxide, toluene, sodium acetate trihydrate, acetic acid, nitric acid and sodium hydroxide were used as received. $Cu(NO_3)_2$, $Ni(NO_3)_2$, $Zn(NO_3)_2$, NH_4Cl, $NH_4(NO_3)$, $K_2(SO_4)$ and $NaH_2(PO_4)$ (Sigma-Aldrich) were used for the cationic and anionic selectivity experiments. 3-Mercaptopropionic acid (3-MPA, Sigma-Aldrich) and Tetramethylammonium hydroxide (TMAOH, Fluka 25 % in water) were used without further purification. High purity water with a resistivity of 18 MΩ cm^{-1} was used throughout all the experiments.

2.2. Characterization techniques for the adsorbent system

SPION and nanoparticle composites (NPCs) synthesized by functionalization of SPION with 3-MPA were imaged with transmission electron microscopy (HR-FEG-TEM, JEOL JEM-2100, Tokyo, Japan). TEM-EDX for chemical composition determination was applied for the nanoparticles in dry form. The stability and the homogeneity of the SPION suspension in hydrodynamic mode were determined by

dynamic light scattering (DLS, Delsa Nano C, Beckman Coulter, Brea, CA, USA). thermogravimetric analysis (TGA, Q5000, TA instruments, New Castle, DE, USA) was employed to measure the weight variation and determine if the particles were loaded with the reagent. Fourier transform infra-red (FTIR, Nicolet Instruments model Avatar-100 equipped with ATR diamond at 303 K, Madison, WI, USA) was used to verify the interaction between SPION, 3-MPA and their bonding before and after the adsorption process [20-22].

2.3.   Synthesis of adsorbent materials

The synthesis procedure of SPION (~ 10 nm) and 3-MPA-coated SPION has been described elsewhere [23]. A stock solution of iron(III) in chloride medium was prepared by dissolving the salt with a deoxygenated 0.2 mol/L HCl aqueous solution. This solution was added to a deoxygenated solution of 0.7 mol/L NH_4OH under mechanical stirring. After a few minutes, the appropriate salt of iron(II) in 2:1 ratio was added to avoid the partial oxidation of Fe(II). The particles were aged in the solution for about 45 min under mechanical stirring and nitrogen bubbling, decanted by magnetic settling, and washed with deoxygenated water several times. A known amount of the synthesized particles was mixed with 3-MPA solution (150 mM) in toluene using a rotary shaker for 24 hours. After phase separation using magnetic settlement, the particles were washed with toluene three times to remove the excess of 3-MPA deposited on the surface of the particles. The particles were dried at room temperature (23 °C). FT-IR was used to check whether the reagent was bound to the surface of the particles, in a wavenumber range 4000-600 cm^{-1} [24,25]. TGA analysis was carried out with heating rate of 10 ºC/min in nitrogen until 900 ºC [26,27].

2.4.   Adsorption and Desorption Experiments

The adsorption experiments were performed by mixing a known amount of 3-MPA-coated SPION with aqueous solutions of As(V) in 0.2 M Acetic acid/Acetate medium using a rotary shaker at room temperature (23 °C). The pH of the solution was controlled using either HNO_3 or NaOH standardized

solutions and confirmed by pH measurements (pH-meter, Crison, Barcelona, Spain). After mixing, the aqueous phase was separated from the solid phase by magnetic settlement and centrifugation at 14000 rpm (Genofuge 16 M, Techne, Prinston, NJ, USA). The concentration of metal ions in the supernatant was determined by inductively coupled plasma atomic emission spectroscopy (ICP-AES, iCAP 6000, Thermo Fisher, Waltham, MA, USA). As(V) adsorption was calculated by mass balance and the effect of different parameters, such as time, pH and initial As(V) concentration were recorded. The dissolution of iron oxide was monitored by determining the concentration of iron in aqueous solutions.

In the desorption experiments, 10 mL of the elution solution (HNO_3 or NaCl) was added to an accurately-measured quantity of 3-MPA-coated SPION loaded with As(V). After 60 minutes of contact at temperature 23 °C, the aqueous and the solid phases were separated by centrifugation and the concentration of As(V) in the supernatant was measured.

The total adsorption capacity was expressed as mmol of Arsenate (or other metal in case of selectivity experiments) per gram of adsorbent system.

2.5. Selectivity Experiments

Two different experiments were performed to study the selectivity of the adsorbent. In one, solutions of As(V) containing metal ions such as Cu(II), Ni(II) and Zn(II) in molar ratios 1:1 and 1:2 (As(V): metal ions) were treated in order to know if the adsorbent system can be used for As(V) removal in the presence of metals. In the other, solutions of As(V) containing 0.25 mol L^{-1} of Cl^-, NO_3^-, SO_4^{2-} or PO_4^{3-} (ratio 20:1 respect of As(V) total in solution) were treated to observe the behaviour of the absorbent system in the presence of interfering anions. The experiments were performed in the same way as the adsorption experiments by mixing a known amount of 3-MPA-coated SPION with the solutions using rotary shaker at room temperature (23 °C). The pH of the solution was controlled using either HNO_3 or NaOH standardized solutions and confirmed by pH measurements (pH-meter, Crison, Barcelona, Spain). After mixing, the aqueous phase was separated from the solid phase and the concentration of metal ions in the supernatant was determined by ICP-AES.

3. Results and discussion

3.1. Characterization of adsorbent material

The amount of 3-MPA coated on the surface of SPION was determined from the percentage mass loss measured by thermogravimetric analysis (TGA/DTG). As shown in Fig. 1, the TGA curve for SPION shows a mass loss over 100–350 °C of about 8%. This is most likely due to the loss of adsorbed water and dehydration of internal OH groups. However, for 3-MPA-coated SPION, the TGA curve shows two mass loss steps. The first mass loss step over 100–180 °C might be due to the loss of residual water adsorbed physically in the sample. The second mass loss over 200–800 °C was due to the decomposition of 3-MPA. Based on the TGA data, the amount of 3-MPA coated on the surface of SPION is determined to be 3.7 mmol/g.

The TEM image of 3-MPA-coated SPION is shown in Fig. 2a. A review of the actual existing literature highlights an optimal particle size range between 8-20 nm for adsorption applications. As it can be observed, the main nanoparticle size obtained by using the described synthesis method has an average size about 15-20 nm [28-30]. Energy Dispersive X-ray (EDX) analysis data (Fig. 2b) show that the main compositions of the sample are Fe, O, and S. The presence of sulphur in the sample is a confirmation of the coating process [31,32].

In order to confirm the coating of the SPION surface with 3-MPA, FT-IR spectrum of SPION, 3-MPA-coated SPION, and 3-MPA were obtained Fig. 3. The FTIR spectrum of 3-MPA (Fig. 3a) has two important functional groups: thiol (SH) and carboxylic (COOH) showing a broad O-H stretch band at 3114-2917 cm^{-1} [33]. The vibration of the –SH group present two peaks at 2664 and 2571 cm^{-1} (slightly observed in 3-MPA-coated SPION). The –COOH group has a stretching vibration of C=O at 1714 cm^{-1} and the stretching vibration for C-O at 1267 cm^{-1} [34,35]. Finally, a band at 951 cm^{-1} is attributed to O-H out of plane wagging [36].

In the spectrum of SPION (Fig. 3b), the band at 732 cm^{-1} is attributed to the Fe-O vibrations [33]. In the FTIR spectrum of the 3-MPA coated SPION (Fig. 3c), there are also new bands at 1521 cm^{-1} and 1386 cm^{-1}, which are assigned to asymmetric and symmetric stretching vibrations of COO$^-$ group and the band attributed to C=O for the carboxyl group and S-H groups of MPA lose intensity [34]. A reasonable conclusion would therefore be that the binding of 3-MPA to SPION occurs primarily through the carboxylic group rather than through the SH group.

3.2. Proposed mechanism of 3MPA-SPION interaction

Taking into account the results obtained from the TGA and FT-IR analysis, a proposed structure for 3MPA-coated SPION at acidic pH can be illustrated below [37]:

$$\tag{1}$$
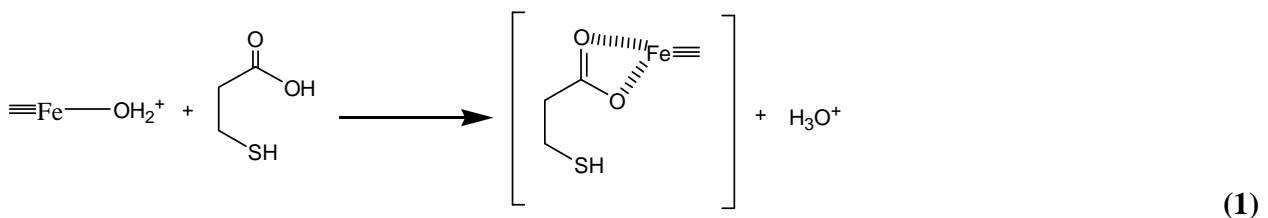
where Fe$\equiv$ represents the SPION.

The presence of a good leaving group such as OH$_2^+$ on the SPION surface when producing the functionalization, is a key factor to this reaction leading an increase in the amount of functionalized Fe atoms on the SPION surface. In this sense, the TGA results corroborate the high degradation of organic compounds between 200 and 800 °C and the TEM-EDX showed quantitatively corresponding amount of sulphur.

3.3. Sorption-desorption properties of As(V) on 3MPA-SPION.

This section includes results of different parameters, i.e., contact time, pH, and As(V) concentration affecting the adsorption process as well as its selectivity against most common interfering ions. The As(V) desorption process is also described.

3.3.1. Effect of the contact time

In these experiments the effect of contact time on the adsorption of As(V) was studied. The experiments were carried out using 10 mg 3-MPA coated SPION at room temperature (23 ºC) and solution pH 4.0 with the contact time varying in the range of 10-360 min. The results obtained are presented in Fig. 4. As can be seen, the 3-MPA-coated SPION synthesized at low pH exhibit high sorption kinetics for As(V) than 3-MPA-coated SPION synthesized at high pH, the 50% of the equilibrium sorption ($t_{1/2}$) being reached in less than 10 minutes. However, to ensure equilibrium, 1 hour contact time was maintained during the extraction studies.

3.3.2. Effect of pH

The adsorption of As(V) (Ci= 100 mg/L) using 3-MPA-coated SPION was investigated by varying the solution pH in the range 2-11 (acetic/acetate media). The results obtained (Fig. 5) revealed that the adsorption of As(V) by 3-MPA-coated SPION is pH dependent. This is in agreement with the results obtained from solvent extraction studies using 3-MPA as extractant [38]. This can be explained by the dependence of the As(V) speciation on the pH.

A comparison of the observed pH effect with that obtained by Muñoz et al. [39] revealed similar behaviour in the adsorption of As(V) by SPION alone with an adsorption maximum at pH 3.8. This similarity supports the conclusion that the arsenic species responsible of the adsorption are the same.

As it is well known, the acidity of arsenate species ($pKa_1 = 2.2$) can be responsible of the observed adsorption, since a relatively high proportion of deprotonated species are present at pH value 3.8 of highest adsorption. For lower pH values (2.0-3.0), the competition of H^+ species for arsenate leads to a lower adsorption. On the other hand, at pH > 5.0 the observed decrease on the As(V) adsorption is due to the increase of OH^- species in suppressing the process (see equation 1).

3.3.3. Effect of Initial As(V) Concentration

In these experiments the effect of the initial As(V) concentration on the sorption of As(V) was studied in order to estimate the maximum loading capacity of 3-MPA-coated SPION. The initial As(V) concentration was in the range of 1.3×10^{-5} mol/L to 1.3×10^{-2} mol/L. The relationship between the equilibrium aqueous concentration and the equilibrium loading capacity for As(V) is shown in Fig. 6. The experimental observations are in good agreement with the Langmuir adsorption model, as follows;

$$q_e = \frac{q_{max} k_L C_e}{1 + k_L C_e} \tag{2}$$

that can be written as:

$$\frac{C_e}{q_e} = \frac{1}{q_{max} k_L} + \frac{C_e}{q_{max}} \tag{3}$$

where q_e is the equilibrium loading capacity (mmol/g), C_e is the equilibrium metal concentration in the aqueous phase (mmol/ L), q_{max} is the maximum loading capacity (mmol/g) corresponding to a monolayer coverage, and k_L is Langmuir constant (L/mmol). The values of the maximum loading of As(V) and Langmuir constant are determined to be 2 mmol/g and 8.3 L/mmol respectively. The maximum loading capacity of As(V) corresponded to 54% (molar basis) of the total binding sites (3.7 mmol 3-MPA/g SPION). The major part of the reagent is likely to be accessible to As(V) ions.

With all parameters optimized, a predicted structure for the compound that exists when As(V) is adsorbed on 3-MPA-coated SPION can be described at pH=4, by the predominant specie of As ($H_2AsO_4^-$) [39,40]:

$$\tag{4}$$
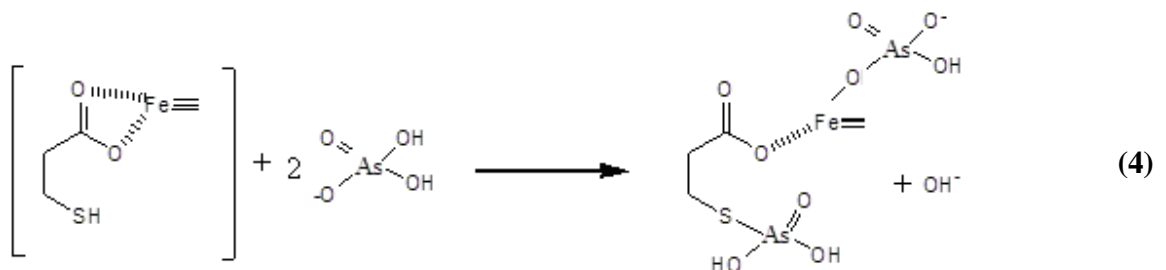
The observed increase of the solution pH supports the appropriateness of the proposed adsorption mechanism by reaction (4).

3.3.4. Selectivity

3.3.4.1. Selectivity with metal ions

In order to examine the separation of As(V) from a mixture containing metals, the selective sorption of As(V) from a solution containing mixture of Cu(II), Zn(II), and Ni(II) was investigated. The results obtained are listed in Table 1. The initial As(V) concentration was 7.5×10^{-4} mol L^{-1}. The results obtained are in agreement with that of solvent extraction studies [41]. It indicates that 3-MPA-coated SPION can be used to extract As(V) selectively from aqueous solutions under the experimental conditions studied.

3.3.4.2. Selectivity with interfering anions

Fig. 7 shows the effect of the pH in the adsorption of As(V) in the pH range 2-11 for the 3-MPA-coated SPION for As(V) solutions with or without anions commonly present in waste waters and potentially interfering in the As(V) adsorption such as chloride, nitrate, sulphate or phosphate. It should be emphasized that the interfering effect of these anions is very significant, given that the As(V)-adsorption capacity in the presence of one of these anions is always lower than the loading capacity without them. But the general tendency of the adsorption capacity to vary with the pH is similar for all interfering anions, with an increase of the loading capacity when the pH increase until 4.5 or 5.0 and stabilization until pH 11.0.

Because of the fact that is not existing a parameter that let us the interfering effect quantification of the different anions, it can be considered the values of loading capacity at pH 4.0 approximately (pH value in the zone where the loading capacity is higher). These values are registered in the Table. 2 with the values of the loading capacity decreasing for each anion.

Selectivity decreases in the order phosphate >> sulphate ~ nitrate ~ chloride. Therefore, the results show that the loading capacity is similar in presence of the all interfering anions except phosphate which present an interfering effect more pronounced. The high interfering effect of phosphate in the loading capacity of As(V) in all pH ranges is due to the effective competition for the Fe(III) centers of the SPION according with the similar affinity of phosphate and arsenate for Fe(III) and due to the major concentration of phosphate in ratio with the arsenate concentration [42].

As it is presented in the literature [10,43], the comparative of the adsorption results between synthetic solution and real water present a greater efficiency for the metal ions removal from synthetic solution and this can be attributed to the matrix effect from real water which increase the ionic strength from solution as well the ions competition by the zeolite adsorption sites. Then, with the interfering anions, ionic strength of real solution has been simulated.

3.3.5. Desorption of As(V)

Different eluting solutions such as HNO_3 and NaCl were employed for the recovery of As(V) from the loaded 3-MPA-coated SPION. The adsorption experiments were performed at pH 3.8 and initial As(V) concentration of 7.5×10^{-4} mol L^{-1}. Corresponding results are 97% for 1.0 M HNO_3 and 5% for 1.0 M NaCl. These results agree with the described pH effect on the adsorption process.

In addition, in the aqueous phases iron is not observed that means no striping of 3-MPA coated SPION is produced. Several 3-MPA-coated SPION samples have been observed by SEM after the desorption process and all of them keep their structure with presence of mercaptopropanoic agent on the SPION surface. That means that the absorbent material is stable after the treatment and it is ready to be used for adsorption – desorption cycles.

3.3.6. Adsorption capacity comparison with similar adsorbent systems.

Comparing the obtained results, as shown by Table 3, with similar studies employing other kind of iron oxides, a high difference adsorption is observed. To explain this behaviour, it must be taken into account that the SPION provide more accessible centres for the arsenate adsorption respect the Fe(III).

3-MPA-coated SPION is around twice more effective for As(V) than SPION. SPION functionalization provides a more active adsorption sites accessible to both arsenite and arsenate. The most important reason for the observed increase of is the decrease of SPION aggregation by a dispersion that leads to a higher availability of adsorption positions [10,44-51].

When the comparison is made with nanoparticles or nanocomposites, something similar happens. The three developed systems, non-supported, modified and Sponge loaded SPION present better adsorption capacity than the reported results in the literature.

4. Conclusions

In this study, the feasibility of using 3-MPA-coated SPION has been demonstrated for the removal of As(V) from diluted nitrate solutions. The time needed to reach maximum adsorption was attained in less than 1 hour and the loading capacity of 3-MPA-coated SPION for As(V) was determined to be 2 mmol/g (150 mg/g). The adsorption behaviour of As(V) at 23 ℃ was similar to Langmuir isotherm. The 3MPA-coated SPION have been shown to be selective for As(V) against base metals such as Cu(II), Zn(II), and Ni(II). FTIR analysis suggested that 3-MPA is bound to the SPION surface through the carboxylic group.

The possibility of combining the superparamagnetic properties of SPION (3-MPA-coated SPION could be separated easily with external magnetic field if leaching is produced) with the selectivity of the reagent (3-MPA) could result in the development of a more effective sorbent for the selective recovery of As(V) from dilute solutions. In this work, sufficiently high loading capacity and high selectivity of As(V) were obtained using 3-MPA coated SPION. As a result, this system provides a ligand exchange mechanism and efficient way to recover As(V) from dilute aqueous solutions. This system might be useful for treatment of process streams of As(V), especially since such streams usually contain low concentrations of these metals.

The experimental results are obtained at laboratory scale, in a pre-stage of pilot plant and for this reason no results at large scale are presented in this paper. Taking into account that it is possible to synthesize nanoparticles at industrial level, next step will be developed in this way.

5. Acknowledgment

6. References

[1] J.M. Azcue, J.O. Nriagu. Arsenic in the environment. Part I: cycling and Characterization. J.O. Nriagu (Ed), John Wiley & Sons, New Cork, 1994, p.1.

[2] W.R. Penrose. CRC Crit. Rev. Environ. Control 4 (1974) 465-482.

[3] USEPA, 2010. Arsenic in drinking water. U. S. Environmental Protection Agency. http://water.epa.gov/lawsregs/rulesregs/sdwa/arsenic/index.cfm (consulted 21/11/13).

[4] T.R.Holm. J Am Water Works Assoc. 94 (4) (2002) 174-181.

[5] E.O. Kartinen, C.J. Martin. Desalination 103 (1995) 79-88.

[6] W. Driehaus, R, Seith, M. Jekel. Water Research 29 (1) (1995) 297-305.

[7] S.R. Chowdhury, E.K. Yanfu. J. Environ. Manage. 91 (2010) 2238-2247.

[8] E. Korngold, N, Belayev, L. Aronov, Desalination, 141(2001) 81-84.

[9] Y. Sato, M, Kang, T, Kamei, Y. Magara. Water Research 36(13) (2002) 3371-3377.

[10] D. Mohan, C.U. Pittman. J. Hazard. Mater. 142(1-2) (2007) 1-53.

[11] O.S. Thirunavukkarasu, T. Viraraghavan, K.S. Subramanian. Water SA 29 (2) (2003) 161-170.

[12] Y. Xu, T. Nakajima, A. Ohki. J. Hazard. Mater. 92 (200) 275-287.

[13] R.W. Siegel, E. Hu, M.C. Rocco. Nanostructure Science and Technology, A worldwide Study, WTEC; Loyola College Kluwer Academic, Baltimore, MD, 1999.

[14] T. Tsakalakos. NATO Sci. Ser., II: Math. Phys. Chem. (Nanostructures: Synthesis, Functional Properties an Applications) 1 (2003) 128.

[15] W. Tungittiplakorn, C. Cohen, L.W. Lion. Environ. Sci. Technol. 39(5) (2005) 1354–1358.

[16] W. Tungittiplakorn, C. Cohen, L.W. Lion, J-Y. Kim. Environ. Sci. Technol. 38(5) (2004) 1605–1610.

[17] K. Wegner. KONA Powder and Particle 29 (2011) 251.

[18] R. Strobel, S.E. Pratsinis. Adv. Powder Technol. 20(2) (2002) 190-194.

[19] L. Mädler, H.K. Kammler, R. Mueller, S.E. Pratsinis, J. Aerosol Sci. 33(2) (2002) 369-289.

[20] N.L. Adolphi, D.L. Huber, J.E. Jaetao, H.C. Bryant, D.M. Lovato, D.L. Fegan, E.L. Venturini, T.C. Monson, T.E. Tessier, H.J. Hathaway, C. Bergemann, R.S. Larson, and E.R. Flynna. J. Magn. Magn. Mater. 321 (2009) 1459-1464.

[21] M. Garza, M. Hinojoza, V. Gonzales. Desarrollo de nanocomposites superparamagneticos de matríz biopolimérica. CIENCIA UANL, (2009) Vol XII (2) (in Spanish).

[22] K-H. Kim, M-J Kim, Y-H. Choa, D-H. Kim, J-H. Yu. IEEE Transition. Magn. 44 (11-1) (2008) 2940-2943.

[23] T. Burks, M. Avila, F. Akhatar, M. Göthelid, P.C. Lansaker, M.S. Toprak, M. Muhammed, A. Uheida. J. Colloid Interf. Sci. 425 (2014) 36-43.

[24] K.G. Ajay, G. Mona, G. Biomaterials 26(13) (2005) 1565-1573.

[25] K. Uzun, E. Çevik, M. Şenel, H. Sözeri, A. Baykal, M. F. Abasıyanık, M. S. Toprak. J. Nanopart. Res. 12(8) (2010) 3057-3067.

[26] M. Mahmoudi, A. Simchi, A.S. Milani, P. Stroeve. J. Colloid Interface Sci. 336 (2009) 510–518.

[27] X. Xuan, Z. Chunfu. J. Nanomater. Article ID 152524, 2011, 7 pages.

[28] H.J. Shipley, S. Yean, A.T. Kan, M.B. Tomson. Environ. Toxicol. Chem. 28(3) (2009) 509–515.

[29] A. Uheida, G. Salazar-Alvarez, E. Björkman, Z. Yu, M. Muhammed. J. Colloid Interf. Sci. 298 (2006) 501-507.

[30] A.B. Chin, I.I. Yacob. J. Mater. Proces. Technol. 191 (2007) 235-237.

[31] L.A. García-Cerda, O.S. Rodríguez-Fernández, R. Betancourt-Galindo, R. Saldívar-Guerrero. Superficies y Vacio 16(1) (2003) 28-31.

[32] J.S. Salazar. Mater. Sci. Eng., C 27 (2007) 1317-1320.

[33] S. Wei, Y. Zhu, Y. Zhang, J. Xu. React. Funct. Polym. 66 (2007) 1272–1277.

[34] O. Taratula, E. Galoppini, D. Wang, D. Chu, Z. Zhang, H. Chen, G. Saraf, Y. Lu, J. Phys. Chem. B 110 (2006) 6506–6515.

[35] M. Hatakeyama, H. Kishi, Y. Kita, K. Imai, K. Nishio, S. Karasawa, Y. Masaike, S. Sakamoto, A. Sandhu, A. Tanimoto, T. Gomi, E. Kohda, M. Abe, H. Handa, J. Mater. Chem. 21 (2011) 5959–5966.

[36] R.A. Nyquist, R.O. Kagel. Infrared spectra of ınorganic compounds. Academic Press, New York, 1971.

[37] T.L. Yun, K. Woo. IEE Trans. nanotechnol. 7(2) (2008) 111-114.

[38] L.M. Rossi, L.L.R. Vono, F.P. Silva, P.K. Kiyohara, E.L. Duarte, J.R. Matos. Appl. Catal., A 330 (2007) 139-144.

[39] J.A. Muñoz, A. Gonzalo, M. Valiente. Environ. Sci. Technol. 36 (2002) 3405-3411.

[40] I. Puigdomemech. Medusa, Royal Institut of Technology, Estocolm, (www.inorg.kth.se). Software, 1999.

[41] A. Uheida, M. Iglesias, C. Fontàs, M. Hidalgo, V. Salvadó, Y. Zhang, M. Muhammed. J. Colloid Interf. Sci. 301 (2006) 402-408.

[42] H. Yan-Chu. Arsenic in the environment. Part I: cycling and Characterization. J.O. Nriagu (Ed), John Wiley & Sons, New Cork, 1994, p.17.

[43] M.R.T. Abreu, F.C.F. Barros, G.S.C. Raulino, C.P. Moura, R.F. Nascimento. Int. J. Civil & Environ. Eng. 12(3) (2012) 20-25.

[44] I. Rau, A. Gonzalo, M. Valiente. React. Funct. Polym. 54 (2003) 85-94.

[45] X.Q. Li, W.X. Zhang. Langmuir 22 (2006) 4638-4642.

[46] T. Pradeep. Thin solid films 517(24) (2009) 6441-6478.

[47] L. Feng. J. Hazard. Mater. 217-218 (2012) 439-446.

[48] S.R. Chowdhury, E.K. Yanfu. J. Environ. Manage. 91 (2010) 2238-2247.

[49] Y. Jin, F. Liu, M Tong, Y. Hou. J.Hazard. Mater. 227-228 (2012) 461-468.

[50] E.A. Deliyanni, D.N. Bakoyannakis, A.I. Zouboulis, K.A. Matis. Chemosphere 50 (2003) 155-163.

[51] T.-H. Hsia, S.-L. Lo, C.-F. Lin, D.-Y. Lee. Coll. Surf. A. 85 (1994) 1-7.